Electronic Supplementary Material (ESI) for Dalton Transactions.

Effect of Ring Size of TMC Ligands in Controlling C-H Bond Reactivity by Metal-Superoxo Species

Monika and Azaj Ansari*

Department of Chemistry, Central University of Haryana, Mahendergarh 123031, India.

Email: ajaz.alam2@gmail.com

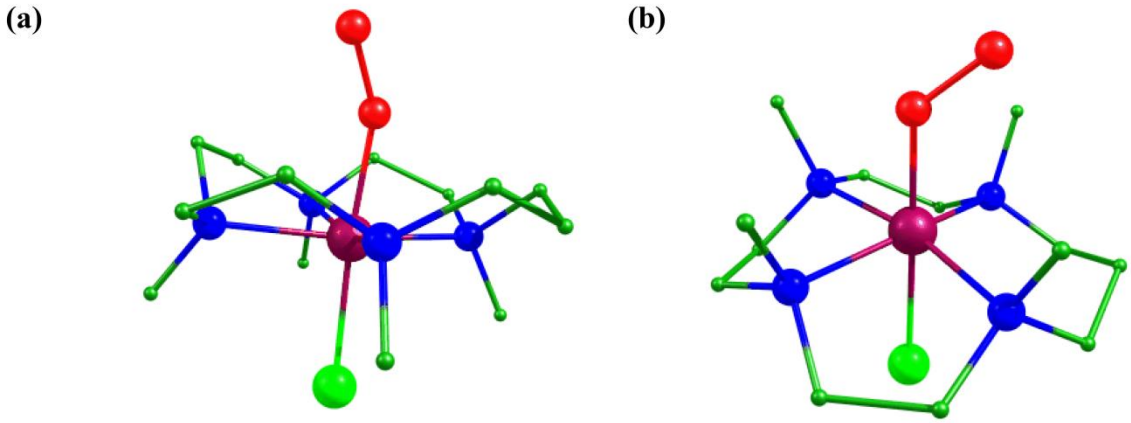

Fig. S1 B3LYP-D2 optimized structures of a) Isomer A and b) Isomer B.

Table S1. B3LYP-D2 computed relative energy (ΔG in kJ mol^{-1}) for species I to IV with both the isomers A and B.

Spin state	13-TMC	14-TMC	
([V(13/14-TMC)O_2Cl]$^+$, I)			
^{4}IA$_{a\text{-}hs}$	43.6	^{4}IA$_{b\text{-}hs}$	51.5
^{2}IA$_{a\text{-}hs}$	0	^{2}IA$_{b\text{-}hs}$	0
^{4}IB$_{a\text{-}hs}$	62.1	^{4}IB$_{b\text{-}hs}$	67.1
^{2}IB$_{a\text{-}hs}$	10.6	^{2}IB$_{b\text{-}hs}$	14.7
([Cr(13/14-TMC)O_2Cl]$^+$, II)			
^{5}IIA$_{a\text{-}hs}$	13.1	^{5}IIA$_{b\text{-}hs}$	16.5
^{3}IIA$_{a\text{-}hs}$	0	^{3}IIA$_{b\text{-}hs}$	0
^{3}IIA$_{a\text{-}ls}$	3.9	^{3}IIA$_{b\text{-}ls}$	4.1
^{1}IIA$_{a\text{-}ls}$	274.1	^{1}IIA$_{b\text{-}ls}$	264.4
^{5}IIB$_{a\text{-}hs}$	28.9	^{5}IIB$_{b\text{-}hs}$	24.9
^{3}IIB$_{a\text{-}hs}$	6.6	^{3}IIB$_{b\text{-}hs}$	5.5
^{3}IIB$_{a\text{-}ls}$	13.7	^{3}IIB$_{b\text{-}ls}$	7.8
^{1}IIB$_{a\text{-}ls}$	273.4	^{1}IIB$_{b\text{-}ls}$	265.5
([Mn(13/14-TMC)O_2Cl]$^+$, III)			
^{6}IIIA$_{a\text{-}hs}$	0	^{6}IIIA$_{b\text{-}hs}$	26.4
^{4}IIIA$_{a\text{-}hs}$	17.2	^{4}IIIA$_{b\text{-}hs}$	0
^{4}IIIA$_{a\text{-}is}$	26.5	^{4}IIIA$_{b\text{-}is}$	86.0
^{2}IIIA$_{a\text{-}is}$	35.3	^{2}IIIA$_{b\text{-}is}$	60.9
^{2}IIIA$_{a\text{-}ls}$	35.2	^{2}IIIA$_{b\text{-}ls}$	63.1
^{6}IIIB$_{a\text{-}hs}$	15.6	^{6}IIIB$_{b\text{-}hs}$	28.6
^{4}IIIB$_{a\text{-}hs}$	30.9	^{4}IIIB$_{b\text{-}hs}$	3.5
^{4}IIIB$_{a\text{-}is}$	61.8	^{4}IIIB$_{b\text{-}is}$	93.9
^{2}IIIB$_{a\text{-}is}$	40.4	^{2}IIIB$_{b\text{-}is}$	65.1
^{2}IIIB$_{a\text{-}ls}$	142.5	^{2}IIIB$_{b\text{-}ls}$	65.0
([Fe(13/14-TMC)O_2Cl]$^+$, IV)			
^{7}IVA$_{a\text{-}hs}$	0	^{7}IVA$_{b\text{-}hs}$	0
^{5}IVA$_{a\text{-}hs}$	20.2	^{5}IVA$_{b\text{-}hs}$	6.8
^{5}IVA$_{a\text{-}is}$	37.5	^{5}IVA$_{b\text{-}is}$	38.8
^{3}IVA$_{a\text{-}is}$	96.4	^{3}IVA$_{b\text{-}is}$	71.7
^{3}IVA$_{a\text{-}ls}$	54.4	^{3}IVA$_{b\text{-}ls}$	43.9
^{1}IVA$_{a\text{-}ls}$	145.6	^{1}IVA$_{b\text{-}ls}$	135.1
^{7}IVB$_{a\text{-}hs}$	27.6	^{7}IVB$_{b\text{-}hs}$	8.2
^{5}IVB$_{a\text{-}hs}$	27.6	^{5}IVB$_{b\text{-}hs}$	18.8
^{5}IVB$_{a\text{-}is}$	40.7	^{5}IVB$_{b\text{-}is}$	75.4
^{3}IVB$_{a\text{-}is}$	62.7	^{3}IVB$_{b\text{-}is}$	56.7
^{3}IVB$_{a\text{-}ls}$	48.9	^{3}IVB$_{b\text{-}ls}$	131.9
^{1}IVB$_{a\text{-}ls}$	136.2	^{1}IVB$_{b\text{-}ls}$	132.0

Table S2. B3LYP-D2 computed formation energies of species I to V with ground state.

Formation energy(kJ/mol)		
Spin State	**13-TMC**	**14-TMC**
$^{2}I_{hs}$	-727.4	-725.5
$^{3}II_{hs}$	-688.2	-670.7
$^{6/4}III_{hs}$	-586.9	-646.0
$^{7}IV_{hs}$	-652.9	-642.7
$^{2}V_{ls}$	-686.1	-1515.1

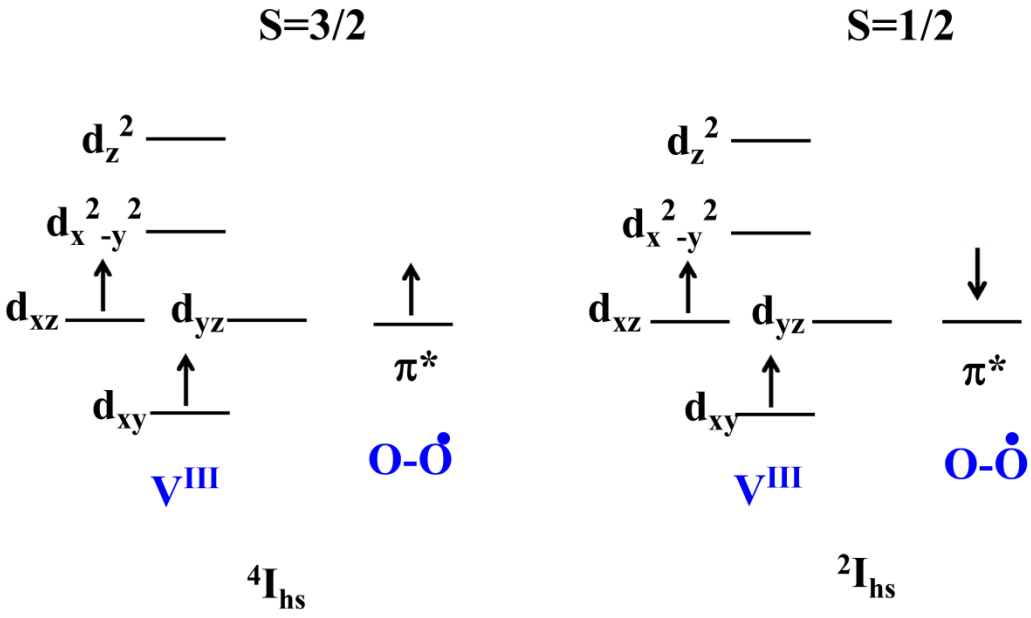

Scheme S1. A model structure of vanadium-superoxo species with existence of quartet, and doublet spin states.

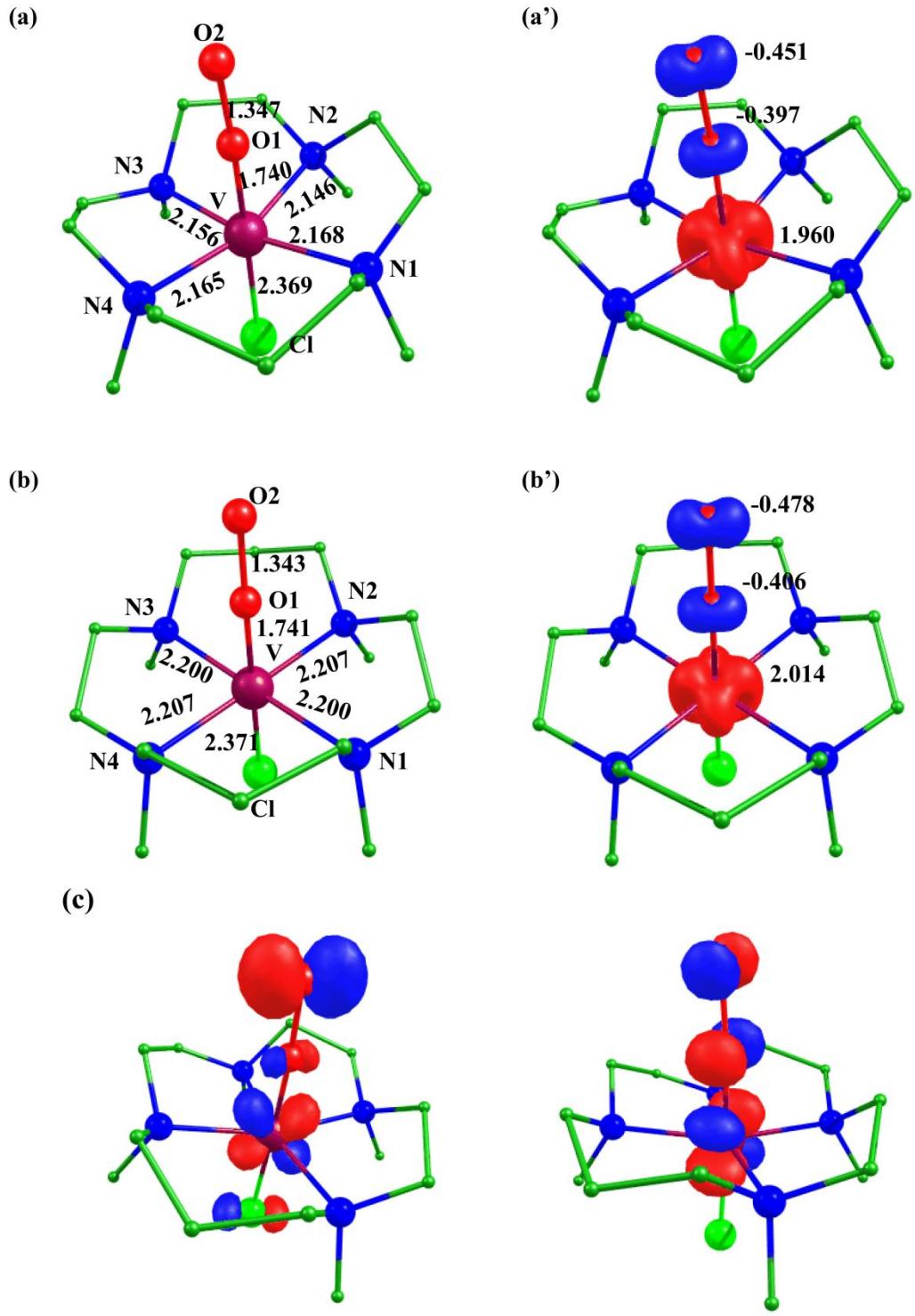

Fig. S2 B3LYP-D2 a) Optimized structure (bond lengths in Å), a') corresponding spin density plot of $^{2}I_{a\text{-}hs}$, b) optimized structure (bond lengths in Å), b') corresponding spin density plot of $^{2}I_{b\text{-}hs}$, and c) $d_{yz/xz}$ orbitals.

Table S3. B3LYP-D2 computed selective structural parameters of metal-superoxo species, intermediates, transition states and product with 13-TMC ligand.

	Bond length (Å)												Bond angle (˚)					
Spin State	M-O1	O1-O2	M-Cl	M-N1	M-N2	M-N3	M-N4	M-N_{avg}	O2-H1	O2-H2	C-H	O2-C2	MO1O2	O1-M-Cl	O2-H1-C1	O2-H2-C2	N4-M-N5	N6-M-N7
									$[V(13\text{-}TMC)O_2Cl]^+$									
$^4I_{a\text{-}hs}$	1.939	1.369	2.378	2.178	2.145	2.149	2.150	2.155	-	-	-	-	141.1	174.9	-	-	167.9	162.1
$^2I_{a\text{-}hs}$	1.740	1.347	2.369	2.168	2.146	2.156	2.165	2.159	-	-	-	-	176.4	176.3	-	-	167.9	164.4
$^4I_{a\text{-}hs}$-ts1	1.871	1.445	2.416	2.150	2.183	2.155	2.149	2.159	1.407	-	1.221	-	136.2	173.8	175.1	-	165.2	167.8
$^2I_{a\text{-}hs}$-ts1	1.867	1.438	2.415	2.152	2.179	2.155	2.153	2.159	1.364	-	1.246	-	138.9	174.9	177.2	-	167.9	165.0
$^4I_{a\text{-}hs}$-Int	1.874	1.516	2.411	2.146	2.186	2.155	2.143	2.157	-	-	-	-	132.8	172.6	-	-	166.2	167.9
$^2I_{als}$-Int	1.648	1.977	2.437	2.134	2.109	2.164	2.165	2.143	-	-	-	-	131.1	131.1	-	-	161.2	162.2
$^4I_{a\text{-}hs}$-ts2	1.781	1.896	2.461	2.180	2.170	2.125	2.154	2.157	-	1.546	-	1.190	135.9	173.5	-	175.7	165.9	169.5
^2I_a-P	1.621	-	2.451	2.162	2.162	2.139	2.148	2.153	-	-	-	-	-	175.7	-	-	166.7	168.2
Ref[1]	1.568	-	-	-	-	-	-	-	-	-	-	-	-	-	-	-	-	-
									$[Cr(13\text{-}TMC)O_2Cl]^+$									
$^5II_{a\text{-}hs}$	2.039	1.372	2.380	2.154	2.106	2.115	2.123	2.124	-	-	-	-	133.9	171.8	-	-	168.7	163.4
$^3II_{a\text{-}hs}$	1.975	1.365	2.386	2.155	2.112	2.116	2.127	2.127	-	-	-	-	135.6	171.5	-	-	168.6	164.4
$^3II_{a\text{-}ls}$	1.906	1.366	2.366	2.153	2.112	2.114	2.125	2.126	-	-	-	-	139.8	172.4	-	-	168.5	164.6
$^1II_{a\text{-}ls}$	1.925	1.364	2.368	2.153	2.109	2.115	2.127	2.126	-	-	-	-	140.2	172.3	-	-	168.6	164.5
$^5II_{a\text{-}hs}$-ts1	1.951	1.452	2.404	2.122	2.155	2.110	2.112	2.125	1.343	-	1.252	-	131.4	173.1	175.6	-	165.5	169.3
$^3II_{a\text{-}hs}$-ts1	1.946	1.447	2.407	2.130	2.155	2.111	2.111	2.127	1.298	-	1.289	-	132.0	171.0	173.8	-	166.0	168.8
$^3II_{a\text{-}ls}$-ts1	1.906	1.446	2.390	2.130	2.156	2.111	2.110	2.127	1.309	-	1.280	-	134.0	171.7	175.1	-	165.9	168.8
$^1II_{a\text{-}ls}$-ts1	1.906	1.446	2.390	2.130	2.156	2.111	2.110	2.127	1.345	-	1.258	-	134.0	171.7		-	165.9	168.8
$^5II_{a\text{-}hs}$-Int	1.739	2.179	2.397	2.160	2.122	2.111	2.115	2.127	-	-	-	-	136.8	174.2	-	-	166.3	168.5
$^3II_{a\text{-}ls}$-Int	1.918	1.518	2.384	2.109	2.113	2.154	2.119	2.124	-	-	-	-	129.7	173.1	-	-	168.6	166.5
$^5II_{a\text{-}hs}$-ts2	1.941	1.749	2.423	2.127	2.139	2.146	2.087	2.125	-	1.557	-	1.192	131.5	172.8	-	177.6	164.7	170.5
$^3II_{a\text{-}ls}$-ts2	1.851	1.668	2.414	2.151	2.152	2.086	2.122	2.128	-	1.766	-	1.144	131.5	169.9	-	1.766	166.2	170.1

$^{3}II_{a\text{-}hs}$-P	1.720	-	2.419	2.137	2.134	2.118	2.123	2.128	-	-	-	-	-	177.0	-	-	165.1	168.8
$^{1}II_{a\text{-}ls}$-P	1.584	-	2.392	2.151	2.151	2.105	2.117	2.131	-	-	-	-	-	176.1	-	-	168.0	170.4
								$[Mn(13\text{-}TMC)O_2Cl]^+$										
$^{6}III_{a\text{-}hs}$	2.284	1.379	2.482	2.137	2.075	2.114	2.096	2.105	-	-	-	-	133.7	175.2	-	-	168.9	159.6
$^{4}III_{a\text{-}hs}$	2.078	1.323	2.352	2.231	2.202	2.237	2.161	2.208	-	-	-	-	133.8	170.7	-	-	163.7	158.6
$^{4}III_{a\text{-}is}$	1.967	1.365	2.336	2.136	2.073	2.082	2.102	2.098	-	-	-	-	135.2	170.9	-	-	169.9	163.8
$^{2}III_{a\text{-}is}$	1.910	1.359	2.327	2.135	2.074	2.085	2.103	2.099	-	-	-	-	138.9	173.3	-	-	170.7	164.8
$^{2}III_{a\text{-}ls}$	1.909	1.359	2.326	2.135	2.074	2.085	2.103	2.099	-	-	-	-	138.9	173.3	-	-	170.7	164.8
$^{6}III_{a\text{-}hs}$-ts1	1.931	1.434	2.344	2.238	2.146	2.241	2.183	2.202	1.358	-	1.251	-	131.6	170.5	172.8	-	165.1	162.5
$^{4}III_{a\text{-}hs}$-ts1	1.938	1.426	2.348	2.193	2.232	2.167	2.230	2.205	1.305	-	1.296	-	131.9	169.1	168.5	-	162.3	165.0
$^{4}III_{a\text{-}is}$-ts1	1.901	1.449	2.353	2.095	2.139	2.075	2.079	2.097	1.360	-	1.244	-	132.0	173.3	175.7	-	166.1	171.1
$^{2}III_{a\text{-}is}$-ts1	1.897	1.443	2.357	2.106	2.140	2.075	2.078	2.099	1.315	-	1.279	-	132.5	171.3	173.3	-	166.9	170.5
$^{2}III_{a\text{-}ls}$-ts1	1.886	1.446	2.358	2.105	2.142	2.075	2.078	2.100	1.330	-	1.266	-	132.9	171.7	175.0	-	166.7	170.5
$^{6}III_{a\text{-}hs}$-Int	2.092	1.521	2.493	2.191	2.066	2.159	2.069	2.121	-	-	-	-	129.3	174.6	-	-	168.6	164.8
$^{4}III_{a\text{-}is}$-Int	1.904	1.524	2.358	2.079	2.133	2.083	2.082	2.094	-	-	-	-	127.7	172.6	-	-	170.2	167.0
$^{2}III_{a\text{-}ls}$-Int	2.256	1.320	2.482	2.137	2.075	2.113	2.096	2.105	-	-	-	-	141.1	170.8	-	-	168.9	159.5
$^{4}III_{a\text{-}is}$-ts2	1.811	1.747	2.399	2.088	2.126	2.130	2.051	2.099	-	1.728	-	1.150	130.2	169.2	-	172.3	166.7	170.9
$^{2}III_{a\text{-}ls}$-ts2	1.839	1.653	2.371	2.090	2.133	2.137	2.050	2.102	-	1.765	-	1.145	132.1	170.5	-	173.5	166.8	171.9
$^{4}III_{a\text{-}hs}$-P	1.686	-	2.415	2.103	2.109	2.085	2.099	2.099	-	-	-	-	-	177.1	-	-	166.0	169.0
$^{2}III_{a\text{-}ls}$-P	1.640	-	2.377	2.114	2.115	2.081	2.092	2.100	-	-	-	-	-	176.6	-	-	166.7	170.2
								$[Fe(13\text{-}TMC)O_2Cl]^+$										
$^{7}IV_{a\text{-}hs}$	2.145	1.322	2.364	2.181	2.172	2.209	2.163	2.181	-	-	-	-	155.5	176.4	-	-	163.3	154.3
$^{5}IV_{a\text{-}hs}$	1.983	1.349	2.352	2.181	2.158	2.186	2.186	2.178	-	-	-	-	147.5	176.6	-	-	164.1	158.2
$^{5}IV_{a\text{-}is}$	2.283	1.359	2.443	2.111	2.046	2.078	2.085	2.080	-	-	-	-	134.8	175.3	-	-	158.5	170.3
$^{3}IV_{a\text{-}is}$	2.175	1.369	2.435	2.125	2.048	2.087	2.084	2.086	-	-	-	-	136.0	175.1	-	-	170.8	160.7
$^{3}IV_{a\text{-}ls}$	1.988	1.363	2.338	2.114	2.053	2.059	2.076	2.075	-	-	-	-	131.2	169.6	-	-	170.4	165.4
$^{1}IV_{a\text{-}ls}$	1.956	1.356	2.345	2.061	2.053	2.112	2.073	2.075	-	-	-	-	131.8	171.7	-	-	166.1	171.1
$^{7}IV_{a\text{-}hs}$-ts1	1.970	1.417	2.390	2.183	2.194	2.201	2.167	2.186	1.341	-	1.263	-	143.8	175.9	178.5	-	164.3	160.3
$^{5}IV_{a\text{-}hs}$-ts1	1.941	1.421	2.385	2.198	2.165	2.182	2.194	2.185	1.334	-	1.263	-	142.0	175.5	177.6	-	160.7	164.4
$^{5}IV_{a\text{-}is}$-ts1	1.950	1.426	2.349	2.145	2.188	2.150	2.209	2.173	1.358	-	1.251	-	129.3	169.2	170.9	-	163.0	165.5
$^{3}IV_{a\text{-}is}$-ts1	1.966	1.417	2.364	2.154	2.184	2.157	2.204	2.175	1.295	-	1.305	-	130.3	168.7	169.2	-	165.6	163.0

$^{3}IV_{a\text{-}ls}$-ts1	1.885	1.449	2.355	2.056	2.069	2.116	2.054	2.074	1.370	-	1.239	-	130.0	173.1	176.1	-	167.6	171.4
$^{1}IV_{a\text{-}ls}$-ts1	1.886	1.448	2.357	2.052	2.075	2.118	2.051	2.074	1.337	-	1.262	-	129.8	171.9	174.8	-	171.4	168.0
$^{7}IV_{a\text{-}hs}$-Int	1.970	1.497	2.376	2.157	2.178	2.192	2.207	2.183	-	-	-	-	138.5	164.0	-	-	160.7	164.0
$^{5}IV_{a\text{-}is}$-Int	2.079	1.518	2.463	2.076	2.129	2.050	2.086	2.085	-	-	-	-	130.1	175.4	-	-	164.5	171.3
$^{3}IV_{a\text{-}ls}$-Int	1.878	1.524	2.345	2.056	2.063	2.111	2.059	2.072	-	-	-	-	127.1	172.7	-	-	171.3	168.5
$^{7}IV_{a\text{-}hs}$-ts2	1.967	1.732	2.408	2.202	2.177	2.185	2.151	2.179	-	1.599	-	1.181	133.6	172.7	-	176.8	161.1	167.5
$^{5}IV_{a\text{-}is}$-ts2	1.929	1.639	2.437	2.176	2.210	2.179	2.186	2.187	-	1.592	-	1.183	139.6	172.6	-	175.1	161.9	166.9
$^{3}IV_{a\text{-}ls}$-ts2	1.816	1.714	2.375	2.107	2.112	2.022	2.063	2.076	-	1.701	-	1.156	132.1	171.3	-	172.5	167.9	172.4
$^{5}IV_{a\text{-}hs}$-P	1.663	-	2.322	2.147	2.169	2.183	2.205	2.176	-	-	-	-	-	176.9	-	-	162.3	165.2
$^{3}IV_{a\text{-}is}$-P	1.663	-	2.364	2.093	2.099	2.053	2.071	2.079	-	-	-	-	-	177.3	-	-	171.0	167.1
$^{1}IV_{a\text{-}ls}$-P	1.674	-	2.353	2.090	2.090	2.058	2.070	2.077	-	-	-	-	-	176.7	-	-	170.7	166.7
$^{2}IV_{a\text{-}ls}$	1.980	1.354	2.349	2.055	2.093	2.027	2.036	2.053	-	-	-	-	130.8	171.4	-	-	166.9	171.6
Exp.[2]		1.34																
								$[Co(13\text{-}TMC)O_2Cl]^+$										
$^{2}V_{a\text{-}ls}$	1.980	1.354	2.349	2.055	2.093	2.026	2.036	2.052	-	-	-	-	130.8	171.4	-	-	166.9	171.6
$^{2}V_{a\text{-}ls}$-ts1	1.953	1.443	2.365	2.026	2.059	2.100	2.024	2.052	1.285	-	1.301	-	128.6	170.3	172.5	-	171.6	168.1
$^{4}V_{a\text{-}is}$-Int	1.999	1.514	2.470	2.158	2.026	2.117	2.020	2.080	-	-	-	-	128.7	174.0	-	-	167.8	170.7
$^{2}V_{a\text{-}ls}$-Int	1.958	1.528	2.340	2.041	2.091	2.023	2.029	2.046	-	-	-	-	124.5	173.1	-	-	168.1	172.4
$^{6}V_{a\text{-}hs}$-ts2	2.008	1.671	2.394	2.174	2.167	2.130	2.188	2.080	-	1.714		1.156	134.1	171.5	174.7	-	159.6	168.8
$^{2}V_{a\text{-}ls}$-ts2	1.901	1.738	2.371	2.135	2.113	2.076	2.087	2.103	-	1.607	-	1.180	128.8	172.5	174.9	-	175.6	175.2
$^{6}V_{a\text{-}hs}$-P	1.921	-	2.334	2.207	2.179	2.183	2.158	2.182	-	-	-	-	175.5	-	-	-	165.4	153.5
$^{4}V_{a\text{-}is}$-P	1.657	-	2.286	2.132	2.193	2.132	2.189	2.161	-	-	-	-	177.1	-	-	-	164.6	168.2
$^{2}V_{a\text{-}ls}$-P	1.853	-	2.351	2.066	2.062	2.024	2.038	2.047	-	-	-	-	178.4	-	-	-	172.1	165.2
Exp.[3]	1.72	-	-	-	-	-	-	2.02	-	-	-	-	-	-	-	-	-	-

Table S4. B3LYP-D2 computed selective structural parameters of metal-superoxo species, intermediates, transition states and product with 14-TMC ligand.

	Bond Length (Å)								Bond Angel (˚)									
Spin State	M-O1	O1-O2	M-Cl	M-N1	M-N2	M-N3	M-N4	M-N_{avg}	O2-H1	O2-H2	H1-C1	H2-C1	MO1O2	O1-M-Cl	O2-H1-C1	O2-H2-C2	N1-M-N2	N3-M-N4
								[V(14-TMC)O_2Cl]$^+$										
$^4I_{b\text{-}hs}$	1.911	1.370	2.382	2.207	2.188	2.197	2.215	2.202	-	-	-	-	140.0	174.3	-	-	173.1	172.7
$^2I_{b\text{-}hs}$	1.741	1.343	2.371	2.200	2.207	2.200	2.207	2.203	-	-	-	-	173.7	176.1	-	-	173.9	173.9
$^4I_{b\text{-}hs}$-ts1	1.858	1.445	2.419	2.193	2.225	2.213	2.184	2.196	1.407	-	1.216	-	135.3	173.4	176.2	-	174.4	174.6
$^2I_{b\text{-}hs}$-ts1	1.856	1.439	2.418	2.225	2.209	2.186	2.196	2.204	1.364	-	1.239	-	137.5	174.6	178.1	-	174.4	174.5
$^4I_{b\text{-}hs}$-Int	1.859	1.515	2.412	2.180	2.217	2.223	2.192	2.203	-	-	-	-	132.3	172.3	-	-	175.4	175.0
$^2I_{b\text{-}ls}$-Int	1.655	1.912	2.443	2.132	2.216	2.219	2.156	2.181	-	-	-	-	129.7	169.1	-	-	176.6	174.4
$^4I_{b\text{-}hs}$-ts2	1.733	2.074	2.464	2.221	2.196	2.204	2.222	2.211	-	1.550	-	1.211	148.6	178.2	-	173.3	176.2	175.7
$^2I_{b\text{-}hs}$-P	1.616	-	2.451	2.193	2.204	2.192	2.205	2.198		-	-	-	-	176.7	-	-	176.2	176.2
								[Cr(14-TMC)O_2Cl]$^+$										
$^5II_{b\text{-}hs}$	2.021	1.371	2.382	2.179	2.167	2.152	2.177	2.169	-	-	-	-	132.4	172.3	-	-	173.3	172.9
$^3II_{b\text{-}hs}$	1.958	1.363	2.388	2.183	2.167	2.154	2.182	2.171	-	-	-	-	134.7	172.4	-	-	173.8	173.6
$^3II_{b\text{-}ls}$	1.889	1.365	2.368	2.180	2.167	2.154	2.183	2.171	-	-	-	-	139.2	173.2	-	-	174.2	174.0
$^1II_{b\text{-}ls}$	1.909	1.363	2.368	2.180	2.155	2.165	2.177	2.169	-	-	-	-	139.7	173.4	-	-	174.0	173.8
Exp.[4]	1.876	1.231	2.316	-	-	-	-	-		-	-	-	146.3	174.5	-	-	-	-
$^5II_{b\text{-}hs}$-ts1	1.937	1.451	2.406	2.186	2.151	2.161	2.189	2.172	1.343	-	1.250	-	130.7	172.3	172.7	-	174.2	174.3
$^3II_{b\text{-}hs}$-ts1	1.930	1.447	2.409	2.189	2.157	2.168	2.181	2.174	1.298	-	1.286	-	131.9	170.9	170.0	-	174.8	174.7
$^3II_{b\text{-}ls}$-ts1	1.914	1.449	2.390	2.150	2.159	2.187	2.181	2.169	1.309	-	1.247	-	133.1	173.1	173.9	-	174.2	174.3
$^1II_{b\text{-}ls}$-ts1	1.888	1.447	2.390	2.184	2.151	2.162	2.187	2.171	1.345	-	1.258	-	134.2	173.1	-	-	174.6	174.8
$^5II_{b\text{-}hs}$-Int	1.943	1.516	2.397	2.147	2.183	2.196	2.161	2.172	-	-	-	-	127.5	172.0	-	-	175.1	174.6
$^3II_{b\text{-}ls}$-Int	1.894	1.518	2.386	2.161	2.144	2.185	2.196	2.171	-	-	-	-	129.2	171.8	-	-	175.3	174.9
$^5II_{b\text{-}hs}$-ts2	1.911	1.754	2.431	2.159	2.159	2.202	2.202	2.180	-	1.561	-	1.194	127.2	176.7	-	179.6	174.5	174.5
$^3II_{b\text{-}ls}$-ts2	1.867	1.706	2.432	2.156	2.155	2.208	2.208	2.182	-	1.683	-	1.163	125.6	175.1	-	179.0	175.1	175.1

$^{3}II_{b\text{-}hs}$-P	1.715	-	2.419	2.167	2.167	2.176	2.176	2.171	-	-	-	-	-	176.8	-	-	174.5	174.5
$^{1}II_{b\text{-}ls}$-P	1.580	-	2.387	2.176	2.182	2.175	2.182	2.179	-	-	-	-	-	176.9	-	-	176.6	176.6
Exp.[5]	1.698	-	2.383											176.8				
								$[Mn(14\text{-}TMC)O_2Cl]^+$										
$^{6}III_{b\text{-}hs}$	2.107	1.355	2.393	2.289	2.292	2.122	2.151	2.213	-	-	-	-	133.2	171.8	-	-	170.5	170.2
$^{4}III_{b\text{-}hs}$	2.043	1.322	2.354	2.254	2.273	2.217	2.268	2.253	-	-	-	-	133.1	171.4	-	-	169.6	170.0
$^{4}III_{b\text{-}is}$	1.966	1.365	2.331	2.162	2.137	2.129	2.153	2.145	-	-	-	-	132.8	171.7	-	-	173.7	173.1
$^{2}III_{b\text{-}is}$	1.918	1.357	2.333	2.158	2.161	2.132	2.139	2.147	-	-	-	-	134.5	172.4	-	-	173.8	174.1
$^{2}III_{b\text{-}ls}$	1.884	1.357	2.328	2.157	2.141	2.134	2.158	2.079	-	-	-	-	139.2	173.8	-	-	174.2	174.01
$^{6}III_{b\text{-}hs}$-ts1	1.922	1.430	2.346	2.257	2.265	2.268	2.219	2.252	1.358	-	1.242	-	130.6	171.3	169.6	-	172.7	172.8
$^{4}III_{b\text{-}hs}$-ts1	1.928	1.423	2.353	2.257	2.253	2.276	2.230	2.254	1.305	-	1.296	-	131.3	169.6	167.2	-	173.1	173.2
$^{4}III_{b\text{-}is}$-ts1	1.886	1.447	2.348	2.166	2.134	2.128	2.166	2.148	1.360	-	1.240	-	131.2	172.5	169.7	-	174.8	174.8
$^{2}III_{b\text{-}is}$-ts1	1.881	1.442	2.354	2.140	2.157	2.169	2.133	2.149	1.315	-	1.275	-	132.4	171.2	169.3	-	175.2	175.1
$^{2}III_{b\text{-}ls}$-ts1	1.869	1.444	2.355	2.136	2.158	2.169	2.134	2.149	1.330	-	1.262	-	133.3	171.6	170.9	-	175.1	175.2
$^{6}III_{a\text{-}hs}$-Int	1.916	1.511	2.344	2.132	2.318	2.179	2.313	2.235	-	-	-	-	127.8	169.9	-	-	173.7	173.7
$^{4}III_{a\text{-}is}$-Int	1.885	1.519	2.351	2.117	2.162	2.175	2.130	2.146	-	-	-	-	127.1	171.2	-	-	175.8	175.3
$^{2}III_{a\text{-}ls}$-Int	1.767	1.537	2.343	2.128	2.173	2.184	2.135	2.155	-	-	-	-	130.1	170.8	-	-	176.7	176.3
$^{4}III_{b\text{-}is}$-ts2	1.839	1.654	2.341	2.304	2.209	2.304	2.184	2.250	-	1.769	-	1.146	130.8	168.6	-	173.6	174.8	173.6
$^{2}III_{b\text{-}ls}$-ts2	1.814	1.641	2.369	2.147	2.155	2.147	2.180	2.157	-	1.800	-	1.141	133.9	169.2	-	178.2	175.7	176.7
$^{4}III_{b\text{-}hs}$-P	1.680	-	2.417	2.134	2.157	2.134	2.157	2.145	-	-	-	-	-	2.417	-	-	175.1	175.1
$^{2}III_{b\text{-}ls}$-P	1.637	-	2.370	2.143	2.154	2.143	2.153	2.148	-	-	-	-	-	2.370	-	-	175.6	175.5
								$[Fe(14\text{-}TMC)O_2Cl]^+$										
$^{7}IV_{b\text{-}hs}$	2.116	1.327	2.371	2.215	2.223	2.224	2.226	2.222	-	-	-	-	148.1	175.6	-	-	167.6	167.9
$^{5}IV_{b\text{-}hs}$	1.950	1.348	2.355	2.221	2.239	2.213	2.237	2.227	-	-	-	-	145.3	176.0	-	-	170.7	170.2
$^{5}IV_{b\text{-}is}$	2.172	1.364	2.444	2.149	2.135	2.152	2.124	2.140	-	-	-	-	134.9	173.6	-	-	171.3	170.8
$^{3}IV_{b\text{-}is}$	2.160	1.304	2.386	2.232	2.181	2.242	2.215	2.217	-	-	-	-	132.6	173.0	-	-	169.8	170.6
$^{3}IV_{b\text{-}ls}$	1.976	1.363	2.339	2.115	2.130	2.136	2.103	2.121	-	-	-	-	129.5	171.3	-	-	174.6	174.1
$^{1}IV_{b\text{-}ls}$	1.929	1.355	2.346	2.112	2.138	2.136	2.106	2.123	-	-	-	-	130.8	171.7	-	-	174.7	174.9
$^{7}IV_{b\text{-}hs}$-ts1	1.942	1.417	2.395	2.224	2.209	2.241	2.252	2.231	1.341	-	1.258	-	142.3	175.9	178.9	-	171.8	171.8
$^{5}IV_{b\text{-}hs}$-ts1	1.916	1.420	2.391	2.252	2.224	2.210	2.235	2.230	1.334	-	1.259	-	141.1	175.5	177.7	-	172.3	172.1

$^{5}IV_{b\text{-}is}$-ts1	1.947	1.420	2.365	2.263	2.207	2.218	2.190	2.219	1.358	-	1.251	-	128.9	170.5	168.6	-	173.7	173.4
$^{3}IV_{b\text{-}is}$-ts1	1.961	1.412	2.377	2.257	2.213	2.225	2.195	2.222	1.295	-	1.306	-	130.5	169.9	167.0	-	173.5	173.8
$^{3}IV_{b\text{-}ls}$-ts1	1.871	1.447	2.351	2.110	2.150	2.137	2.103	2.125	1.370	-	1.232	-	129.0	172.2	167.0	-	175.7	175.3
$^{1}IV_{b\text{-}ls}$-ts1	1.867	1.447	2.354	2.105	2.111	2.139	2.146	2.125	1.337	-	1.257	-	129.3	171.2	170.5	-	175.9	175.7
$^{7}IV_{b\text{-}hs}$-Int	1.953	1.495	2.378	2.209	2.229	2.247	2.231	2.229	-	-	-	-	134.8	173.5	-	-	173.0	172.4
$^{5}IV_{b\text{-}is}$-Int	2.021	1.514	2.457	2.124	2.166	2.151	2.156	2.149	-	-	-	-	130.6	130.6	-	-	174.5	174.3
$^{3}IV_{b\text{-}ls}$-Int	1.858	1.522	2.344	2.137	2.157	2.106	2.108	2.127	-	-	-	-	126.5	171.4	-	-	176.4	175.9
$^{7}IV_{b\text{-}hs}$-ts2	1.927	1.724	2.403	2.209	2.229	2.260	2.237	2.233	-	1.604	-	1.180	134.4	172.9	-	174.7	173.6	172.6
$^{5}IV_{b\text{-}is}$-ts2	1.802	1.716	2.369	2.100	2.109	2.160	2.142	2.128	-	1.699	-	1.159	130.7	172.0	-	170.8	175.7	176.2
$^{3}IV_{b\text{-}ls}$-ts2	1.802	1.716	2.369	2.100	2.109	2.160	2.142	2.128	-	1.699	-	1.158	130.7	172.0	-	170.7	176.2	175.7
$^{5}IV_{b\text{-}hs}$-P	1.659	-	2.327	2.202	2.202	2.238	2.237	2.219	-	-	-	-	-	177.5	-	-	173.4	173.4
$^{3}IV_{b\text{-}is}$-P	1.657	-	2.362	2.195	2.235	2.207	2.242	2.219	-	-	-	-	-	178.1	-	-	175.4	175.4
$^{1}IV_{b\text{-}ls}$-P	1.669	-	2.347	2.119	2.128	2.119	2.128	2.123	-	-	-	-	-	176.9	-	-	175.3	175.3
Exp.[6]	1.646	-	-	2.067	2.069	2.109	2.117	-	-	-	-	-	-	-	-	-	-	-
								$[Co(14\text{-}TMC)O_2Cl]^+$										
$^{2}V_{b\text{-}ls}$	1.959	1.351	2.348	2.116	2.114	2.116	2.086	2.116	-	-	-	-	129.4	171.6	-	-	174.9	175.1
$^{2}V_{b\text{-}ls}$-ts1	1.939	1.443	2.359	2.089	2.112	2.127	2.083	2.103	1.310	-	1.296	-	127.7	170.4	172.5	-	175.4	175.7
$^{6}V_{b\text{-}hs}$-Int	1.984	1.472	2.415	2.180	2.221	2.216	2.209	2.206					132.1	171.4	-	-	174.0	173.3
$^{4}V_{b\text{-}is}$-Int	1.917	1.511	2.384	2.063	2.243	2.117	2.235	2.164					128.6	172.0	-	-	175.6	175.2
$^{2}V_{b\text{-}ls}$-Int	1.934	1.525	2.342	2.080	2.133	2.114	2.073	2.100	-	-	-	-	123.9	171.2	-	-	176.2	175.7
$^{6}V_{b\text{-}hs}$-ts2	1.949	1.670	2.392	2.193	2.209	2.223	2.239	2.216		1.706		1.157	133.4	171.2	-	-	173.4	173.2
$^{2}V_{b\text{-}ls}$-ts2	1.926	1.736	2.375	2.073	2.083	2.001	2.044	2.050	-	1.612	-	1.176	130.1	172.4	-	175.5	167.0	172.9
$^{6}V_{b\text{-}hs}$-P	1.872	-	2.374	2.221	2.225	2.221	2.226	2.223	-	-	-	-	-	174.4	-	-	170.9	170.9
$^{4}V_{b\text{-}is}$-P	1.647	-	2.284	2.199	2.221	2.199	2.221	2.210	-	-	-	-	-	177.5	-	-	173.9	173.8
$^{2}V_{b\text{-}ls}$-P	1.835	-	2.353	2.090	2.098	2.090	2.099	2.094	-	-	-	-	-	177.4	-	-	173.7	173.7

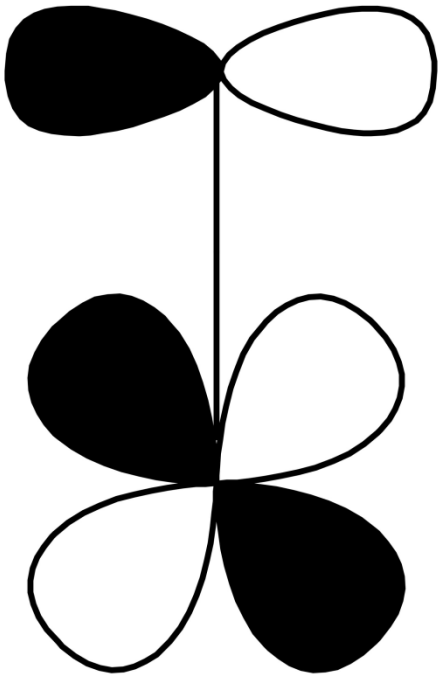

Scheme S2. Orbital picture of vanadium-superoxo species.

Table S5. B3LYP-D2 computed spin density values of metal-superoxo species, intermediates, transition states and product with 13-TMC.

Spin State	M	O1	O2	C1	C2
$[V(13\text{-}TMC)O_2Cl]^+$					
$^4I_{a\text{-}hs}$	2.143	0.236	0.699	-	-
$^2I_{a\text{-}hs}$	1.960	-0.397	-0.451	-	-
$^4I_{a\text{-}hs}$-ts1	2.150	-0.011	0.477	0.264	-
$^2I_{a\text{-}hs}$-ts1	2.162	-0.153	-0.380	-0.283	-
$^4I_{a\text{-}hs}$-Int	2.121	-0.091	0.076	-	-
$^2I_{als}$-Int	0	0	0	-	-
$^4I_{a\text{-}hs}$-ts2	1.985	0.218	0.348	-	0.049
^2I_a-P	1.267	-0.195	-	-	-
$[Cr(13\text{-}TMC)O_2Cl]^+$					
$^5II_{a\text{-}hs}$	3.219	0.317	0.643	-	-
$^3II_{a\text{-}hs}$	3.221	-0.397	-0.627	-	-
$^3II_{a\text{-}ls}$	1.161	0.308	0.606	-	-
$^1II_{a\text{-}ls}$	1.117	-0.383	-0.648	-	-
$^5II_{a\text{-}hs}$-ts1	3.170	0.079	0.431	0.301	-
$^3II_{a\text{-}hs}$-ts1	3.173	-0.106	-0.34	-0.327	-
$^3II_{a\text{-}ls}$-ts1	1.169	-0.017	0.383	0.319	-
$^1II_{a\text{-}ls}$-ts1	-1.116	0.102	0.403	0.297	-
$^5II_{a\text{-}hs}$-Int	1.137	-0.067	0.0136	-	-
$^3II_{a\text{-}ls}$-Int	1.137	-0.067	0.013	-	-
$^5II_{a\text{-}hs}$-ts2	3.149	0.376	0.001	-	-0.118
$^3II_{a\text{-}ls}$-ts2	1.195	0.219	-0.107	-	0.115
$^3II_{a\text{-}hs}$-P	2.761	-0.566	-	-	-
$^1II_{a\text{-}ls}$-P	0	0	-	-	-
$[Mn(13\text{-}TMC)O_2Cl]^+$					
$^6III_{a\text{-}hs}$	4.102	0.467	0.637	-	-
$^4III_{a\text{-}hs}$	4.336	-0.621	-0.765	-	-
$^4III_{a\text{-}is}$	2.165	0.353	0.613	-	-
$^2III_{a\text{-}is}$	-0.006	0.353	0.641	-	-
$^2III_{a\text{-}ls}$	-0.007	0.353	0.641	-	-
$^6III_{a\text{-}hs}$-ts1	4.100	-0.030	0.371	0.282	-
$^4III_{a\text{-}hs}$-ts1	4.149	-0.244	-0.384	-0.324	-
$^4III_{a\text{-}is}$-ts1	2.087	0.1066	0.435	0.288	-
$^2III_{a\text{-}is}$-ts1	2.092	-0.064	-0.349	-0.316	-
$^2III_{a\text{-}ls}$-ts1	0.086	0.003	0.392	0.306	-
$^6III_{a\text{-}hs}$-Int	3.998	0.083	0.027	-	-

$^{4}III_{a\text{-}is}$-Int	2.093	0.038	0.017	-	-
$^{2}III_{a\text{-}ls}$-Int	0	-	-	-	-
$^{4}III_{a\text{-}is}$-ts2	2.194	0.329	-0.160	-	-0.112
$^{2}III_{a\text{-}ls}$-ts2	0.037	0.297	-0.079	-	-0.113
$^{4}III_{a\text{-}hs}$-P	2.625	0.555	-	-	-
$^{2}III_{a\text{-}ls}$-P	1.083	0.012	-	-	-
$[Fe(13\text{-}TMC)O_2Cl]^{+}$					
$^{7}IV_{a\text{-}hs}$	3.903	0.687	0.810	-	-
$^{5}IV_{a\text{-}hs}$	3.938	-0.106	-0.512	-	-
$^{5}IV_{a\text{-}is}$	2.861	0.542	0.687	-	-
$^{3}IV_{a\text{-}is}$	3.448	-0.705	-0.842	-	-
$^{3}IV_{a\text{-}ls}$	1.179	0.329	0.628	-	-
$^{1}IV_{a\text{-}ls}$	1.233	-0.402	-0.664	-	-
$^{7}IV_{a\text{-}hs}$-ts1	3.923	0.429	0.502	0.301	-
$^{5}IV_{a\text{-}hs}$-ts1	3.932	0.232	-0.251	-0.300	-
$^{5}IV_{a\text{-}is}$-ts1	3.115	-0.040	0.315	0.275	-
$^{3}IV_{a\text{-}is}$-ts1	3.198	-0.290	-0.433	-0.331	-
$^{3}IV_{a\text{-}ls}$-ts1	1.028	0.142	0.432	0.282	-
$^{1}IV_{a\text{-}ls}$-ts1	1.038	-0.014	-0.389	-0.302	-
$^{7}IV_{a\text{-}hs}$-Int	3.971	0.269	0.052	-	-
$^{5}IV_{a\text{-}is}$-Int	2.835	0.180	0.023	-	-
$^{3}IV_{a\text{-}ls}$-Int	1.038	0.078	0.001	-	-
$^{7}IV_{a\text{-}hs}$-ts2	3.965	0.692	0.008	-	0.084
$^{5}IV_{a\text{-}is}$-ts2	3.851	0.102	0.025	-	-0.052
$^{3}IV_{a\text{-}ls}$-ts2	1.045	0.408	-0.086	-	0.081
$^{5}IV_{a\text{-}hs}$-P	3.052	0.638	-	-	-
$^{3}IV_{a\text{-}is}$-P	1.288	0.796	-	-	-
$^{1}IV_{a\text{-}ls}$-P	0	0	-	-	-
$[Co(13\text{-}TMC)O_2Cl]^{+}$					
$^{2}V_{a\text{-}ls}$	-0.127	0.449	0.638	-	-
$^{2}V_{a\text{-}ls}$-ts1	-0.011	0.119	0.349	0.332	-
$^{6}V_{a\text{-}hs}$-Int	1.775	0.196	0.014	-	-
$^{2}V_{a\text{-}ls}$-Int	0	0	-	-	-
$^{6}V_{a\text{-}hs}$-ts2	2.736	0.856	0.061	-	-0.115
$^{2}V_{a\text{-}ls}$-ts2	0.059	0.364	-0.084	-	-0.122
$^{6}V_{a\text{-}hs}$-P	2.734	1.396	-	-	-
$^{4}V_{a\text{-}is}$-P	1.831	0.900	-	-	-
$^{2}V_{a\text{-}ls}$-P	-0.028	0.972	-	-	-

Table S6. B3LYP-D2 computed spin density values of metal-superoxo species, intermediates, transition states and product with 14-TMC.

Spin State	M	O1	O2	C1	C2
$[V(14\text{-}TMC)O_2Cl]^+$					
$^4I_{b\text{-}hs}$	2.166	0.203	0.722	-	-
$^2I_{b\text{-}hs}$	2.014	-0.406	-0.478	-	-
$^4I_{b\text{-}hs}$-ts1	2.168	-0.020	0.484	0.256	-
$^2I_{b\text{-}hs}$-ts1	2.181	-0.155	-0.386	-0.272	-
$^4I_{b\text{-}hs}$-Int	2.1371	0.079	-0.096	-	-
$^2I_{b\text{-}ls}$-Int	0	0	0	-	-
$^4I_{b\text{-}hs}$-ts2	1.919	0.175	0.685	-	-0.029
$^2I_{b\text{-}hs}$-P	1.288	-.2004	-	-	-
$[Cr(14\text{-}TMC)O_2Cl]^+$					
$^5II_{b\text{-}hs}$	3.248	0.307	0.650	-	-
$^3II_{b\text{-}hs}$	3.246	-0.390	-0.632	-	-
$^3II_{b\text{-}ls}$	1.185	0.299	0.607	-	-
$^1II_{b\text{-}ls}$	1.132	-0.375	-0.650	-	-
$^5II_{b\text{-}hs}$-ts1	3.192	0.079	0.432	0.295	-
$^3II_{b\text{-}hs}$-ts1	3.191	-0.096	-0.346	-0.322	-
$^3II_{b\text{-}ls}$-ts1	0.945	0.155	0.429	0.291	-
$^1II_{b\text{-}ls}$-ts1	-1.116	0.101	0.403	0.297	-
$^5II_{b\text{-}hs}$-Int	3.179	-0.002	0.040	-	-
$^3II_{b\text{-}ls}$-Int	1.126	-0.044	0.007	-	-
$^5II_{b\text{-}hs}$-ts2	3.159	0.384	0.014	-	-0.118
$^3II_{b\text{-}ls}$-ts2	3.099	-0.266	0.099	-	0.126
$^3II_{b\text{-}hs}$-P	2.784	-0.569	-	-	-
$^1II_{b\text{-}ls}$-P	0	0	-	-	-
$[Mn(14\text{-}TMC)O_2Cl]^+$					
$^6III_{b\text{-}hs}$	4.202	0.287	0.563	-	-
$^4III_{b\text{-}hs}$	4.344	-0.604	-0.776	-	-
$^4III_{b\text{-}is}$	2.176	0.331	0.640	-	-
$^2III_{b\text{-}is}$	2.186	-0.639	-0.377	-	-
$^2III_{b\text{-}ls}$	-0.012	0.350	0.647	-	-
$^6III_{b\text{-}hs}$-ts1	4.144	-0.044	0.359	0.266	-
$^4III_{b\text{-}hs}$-ts1	4.186	-0.248	-0.392	-0.320	-
$^4III_{b\text{-}is}$-ts1	2.095	0.109	0.441	0.279	-
$^2III_{b\text{-}is}$-ts1	2.092	-0.051	-0.347	-0.309	-
$^2III_{b\text{-}ls}$-ts1	0.101	-0.014	0.395	0.299	-
$^6III_{b\text{-}hs}$-Int	3.987	-0.010	0.042	-	-
$^4III_{b\text{-}is}$-Int	2.098	0.042	0.023	-	-

$^{2}III_{b\text{-}ls}$-Int	0	0	0	-	-
$^{4}III_{b\text{-}is}$-ts2	3.898	-0.214	0.049	-	0.113
$^{2}III_{b\text{-}ls}$-ts2	0.063	0.251	-0.054	-	-0.109
$^{4}III_{b\text{-}hs}$-P	2.677	0.545	-	-	-
$^{2}III_{b\text{-}ls}$-P	1.165	-0.061	-	-	-
$[Fe(14\text{-}TMC)O_2Cl]^{+}$					
$^{7}IV_{b\text{-}hs}$	3.929	0.656	0.799	-	-
$^{5}IV_{b\text{-}hs}$	3.937	-0.079	-0.521	-	-
$^{5}IV_{b\text{-}is}$	2.861	0.542	0.687	-	-
$^{3}IV_{b\text{-}is}$	3.426	-0.834	-0.689	-	-
$^{3}IV_{b\text{-}ls}$	1.179	0.329	0.628	-	-
$^{1}IV_{b\text{-}ls}$	1.233	-0.402	-0.664	-	-
$^{7}IV_{b\text{-}hs}$-ts1	3.930	0.432	0.504	0.292	-
$^{5}IV_{b\text{-}hs}$-ts1	3.938	0.247	-0.253	-0.294	-
$^{5}IV_{b\text{-}is}$-ts1	3.194	-0.076	0.277	0.266	-
$^{3}IV_{b\text{-}is}$-ts1	3.262	-0.307	-0.447	-0.327	-
$^{3}IV_{b\text{-}ls}$-ts1	1.031	0.150	0.437	0.269	-
$^{1}IV_{b\text{-}ls}$-ts1	1.036	0.003	-0.391	-0.295	-
$^{7}IV_{b\text{-}hs}$-Int	3.980	0.276	0.051	-	-
$^{5}IV_{b\text{-}is}$-Int	2.896	0.194	0.030	-	-
$^{3}IV_{b\text{-}ls}$-Int	1.039	0.089	-0.000	-	-
$^{7}IV_{b\text{-}hs}$-ts2	3.961	0.698	0.038	-	-0.118
$^{5}IV_{b\text{-}is}$-ts2	1.049	0.419	-0.080	-	-0.119
$^{3}IV_{b\text{-}ls}$-ts2	1.049	0.419	-0.080	-	-0.118
$^{5}IV_{b\text{-}hs}$-P	3.081	0.632	-	-	-
$^{3}IV_{b\text{-}is}$-P	1.313	0.793	-	-	-
$^{1}IV_{b\text{-}ls}$-P	0	0	-	-	-
$[Co(14\text{-}TMC)O_2Cl]^{+}$					
$^{2}V_{b\text{-}ls}$	-0.146	0.456	0.642	-	-
$^{2}V_{b\text{-}ls}$-ts1	0.002	0.107	0.349	-	-
$^{6}V_{b\text{-}hs}$-Int	2.776	0.437	0.083	-	-
$^{4}V_{b\text{-}is}$-Int	1.829	0.173	0.013	-	-
$^{2}V_{b\text{-}ls}$-Int	0	0	0	-	-
$^{6}V_{b\text{-}hs}$-ts2	2.755	0.821	0.070	-	-0.114
$^{2}V_{b\text{-}ls}$-ts2	0.061	0.368	-0.077	-	-0.122
$^{6}V_{b\text{-}hs}$-P	2.750	1.400	-	-	-
$^{4}V_{b\text{-}is}$-P	1.855	0.884	-	-	-
$^{2}V_{b\text{-}ls}$-P	-0.026	0.974	-	-	-

Table S7. B3LYP-D2 computed Mulliken charge at selected atoms with 13/14-TMC ring.

O2 (at distal oxygen)	O2 (at distal oxygen)
$[V(13\text{-}TMC)O_2Cl]^+$	$[V(14\text{-}TMC)O_2Cl]^+$
-0.211	-0.206
$[Cr(13\text{-}TMC)O_2Cl]^+$	$[Cr(14\text{-}TMC)O_2Cl]^+$
-0.166	-0.160
$[Mn(14\text{-}TMC)O_2Cl]^+$	$[Mn(14\text{-}TMC)O_2Cl]^+$
-0.203	-0.086
$[Fe(14\text{-}TMC)O_2Cl]^+$	$[Fe(14\text{-}TMC)O_2Cl]^+$
-0.096	-0.099
$[Co(14\text{-}TMC)O_2Cl]^+$	$[Co(14\text{-}TMC)O_2Cl]^+$
-0.164	-0.159

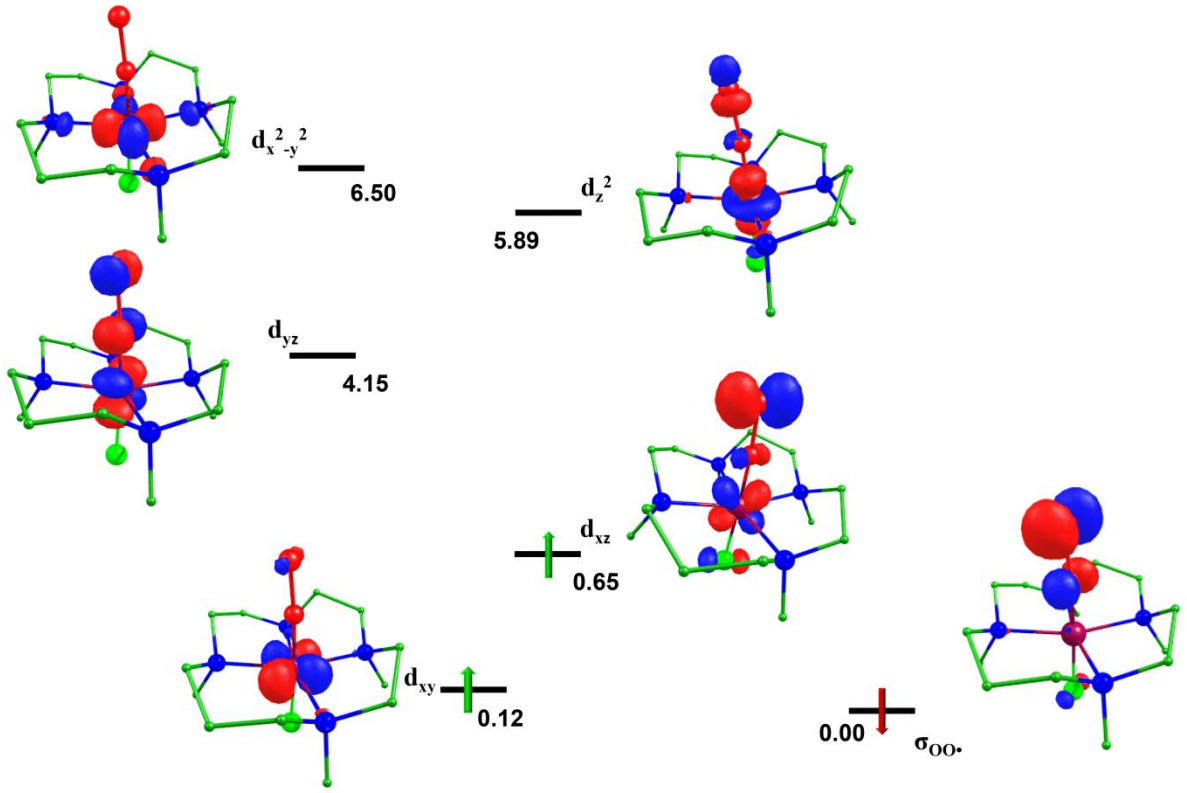

Fig. S3 Computed eigenvalue plot incorporating energies computed for *d* based orbitals for alpha and beta spin corresponding to the ground state ($^2I_{a\text{-}hs}$) of vanadium-superoxo species (energies are given in eV).

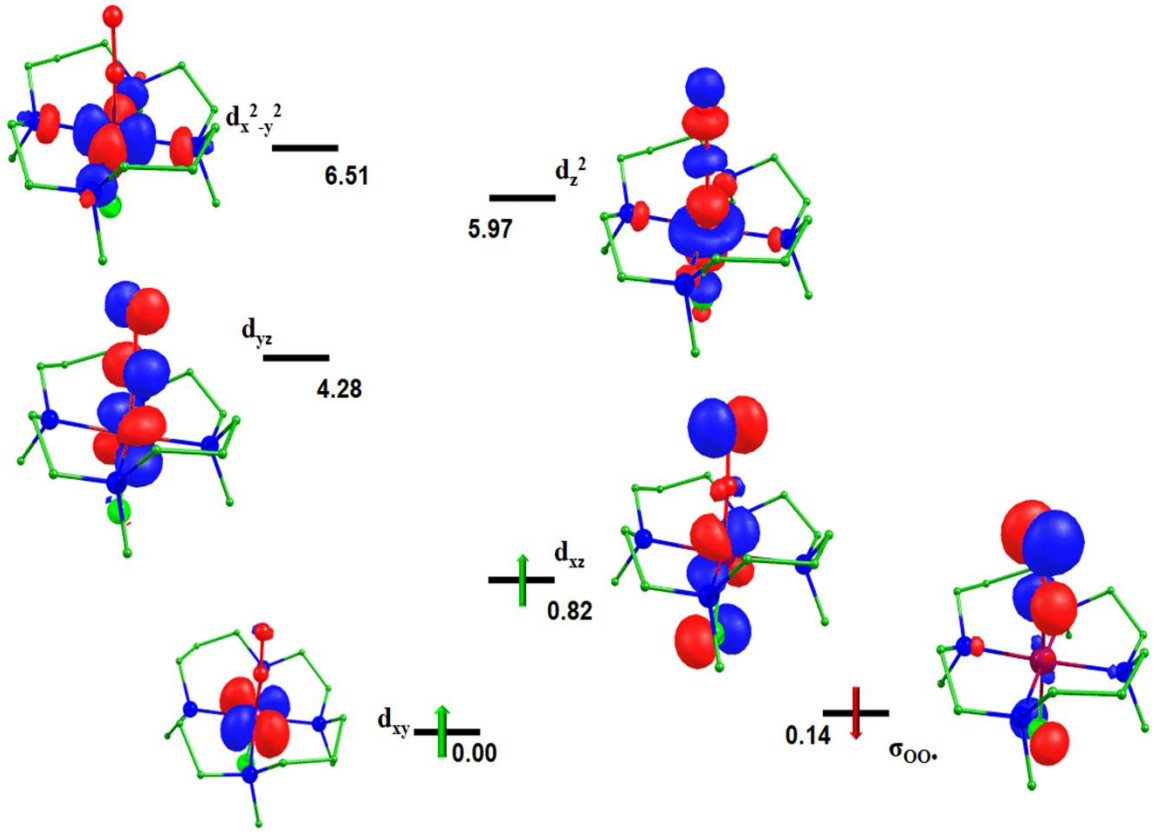

Fig. S4 Computed eigenvalue plot incorporating energies computed for *d* based orbitals for alpha and beta spin corresponding to the ground state ($^2I_{b\text{-}hs}$) of the vanadium-superoxo species (energies are given in eV).

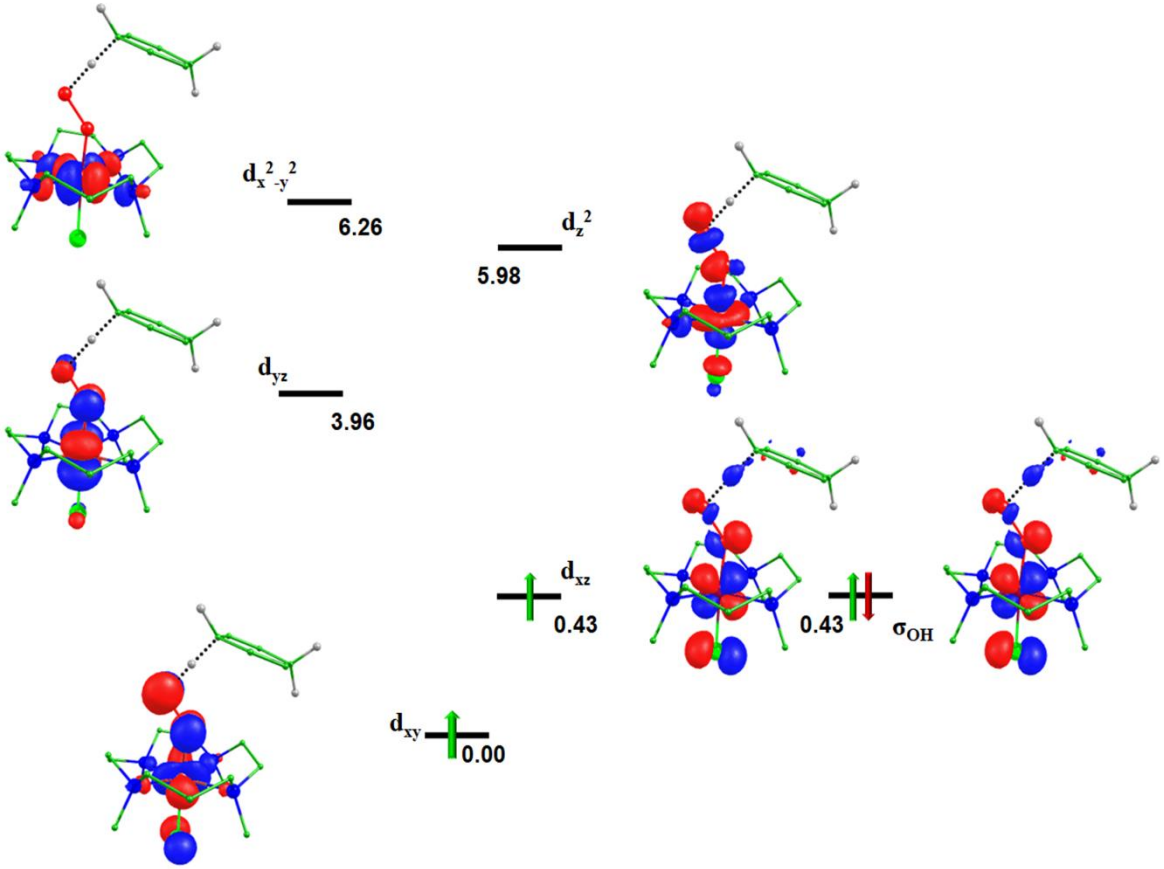

Fig. S5 Computed eigenvalue plot incorporating energies computed for *d* based orbitals for alpha and beta spin corresponding to the ground state ($^2I_{a\text{-}hs}$-ts1) of vanadium-superoxo species (energies are given in eV).

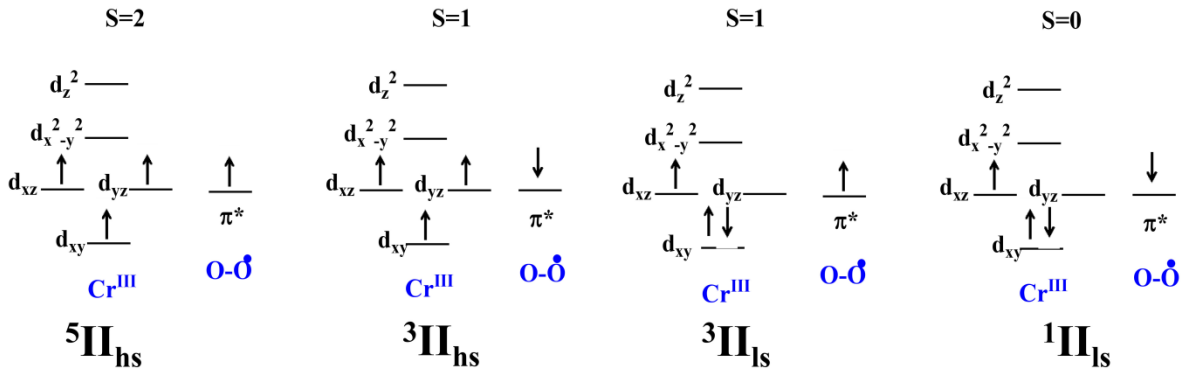

Scheme S3. A model structure of chromium-superoxo species with existence of quintet, triplet and singlet spin states.

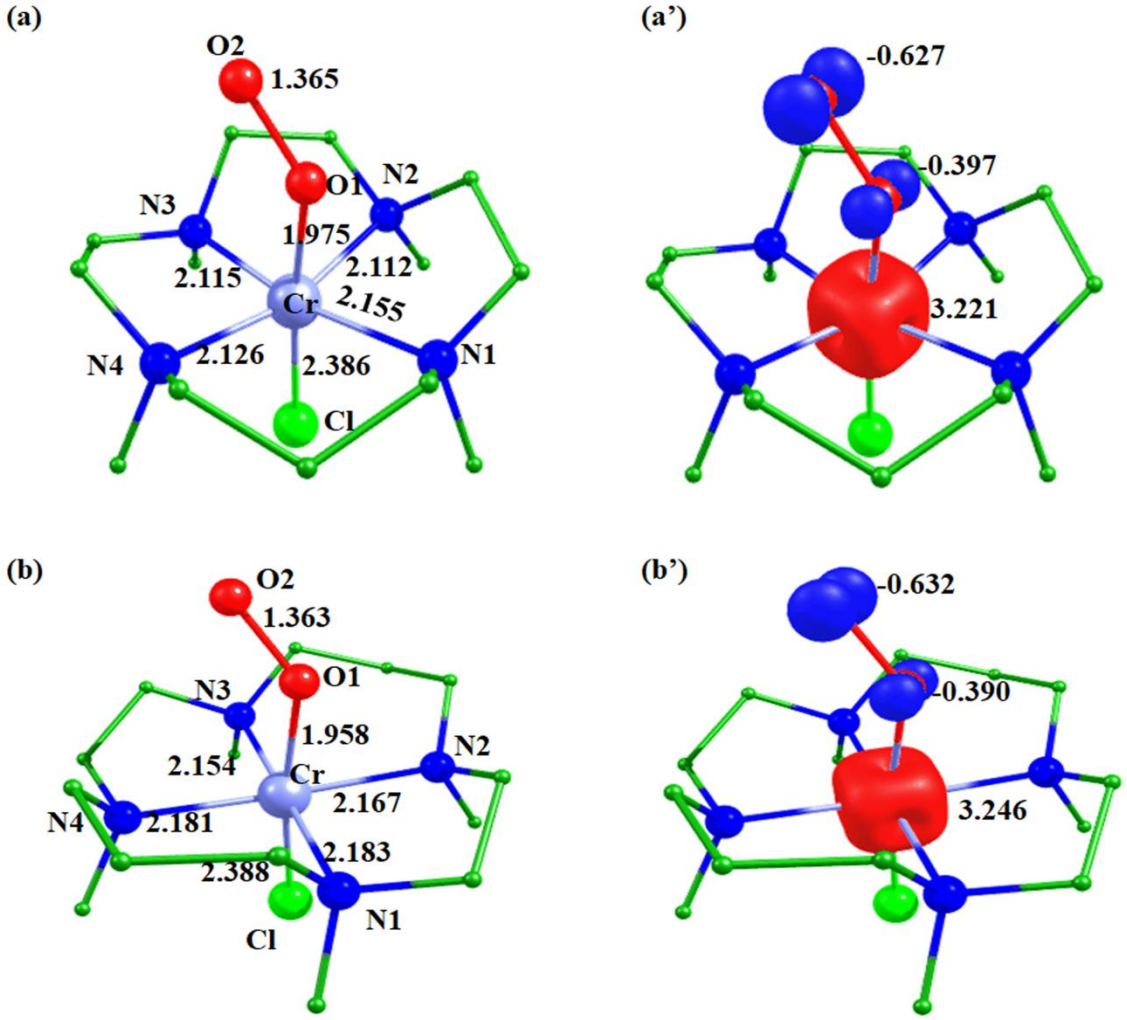

Fig. S6 B3LYP-D2 a) optimized structure (bond lengths in Å), a') corresponding spin density plot of the ground state $^{2}II_{a\text{-}hs}$, b) optimized structure (bond lengths in Å) and b') corresponding spin density plot of the ground state $^{2}II_{b\text{-}hs}$.

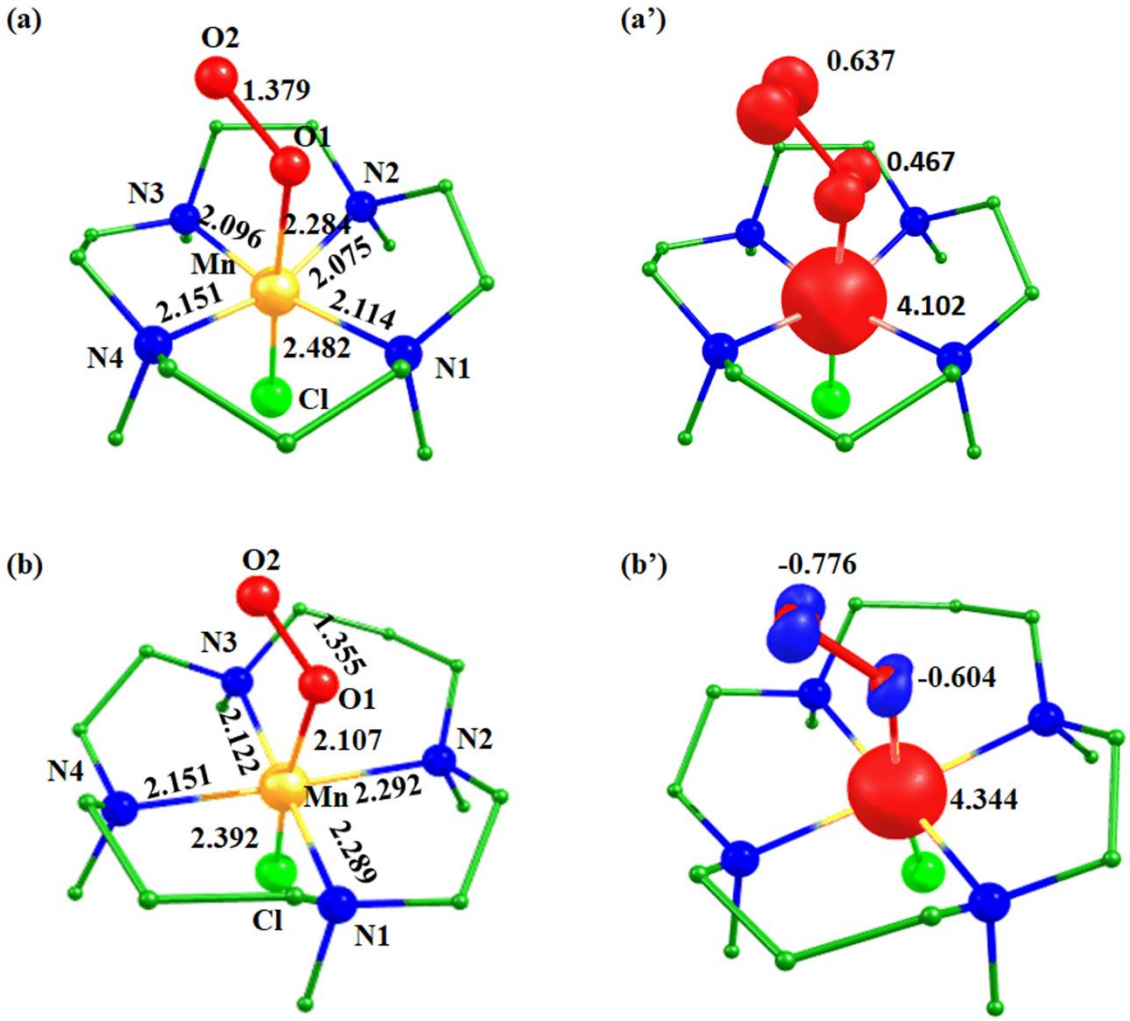

Fig. S7 B3LYP-D2 a) optimized structure (bond lengths in Å), a') corresponding spin density plot of $^{6}III_{a\text{-}hs}$, b) optimized structure (bond lengths in Å) and b') corresponding spin density plot of $^{4}III_{b\text{-}hs}$.

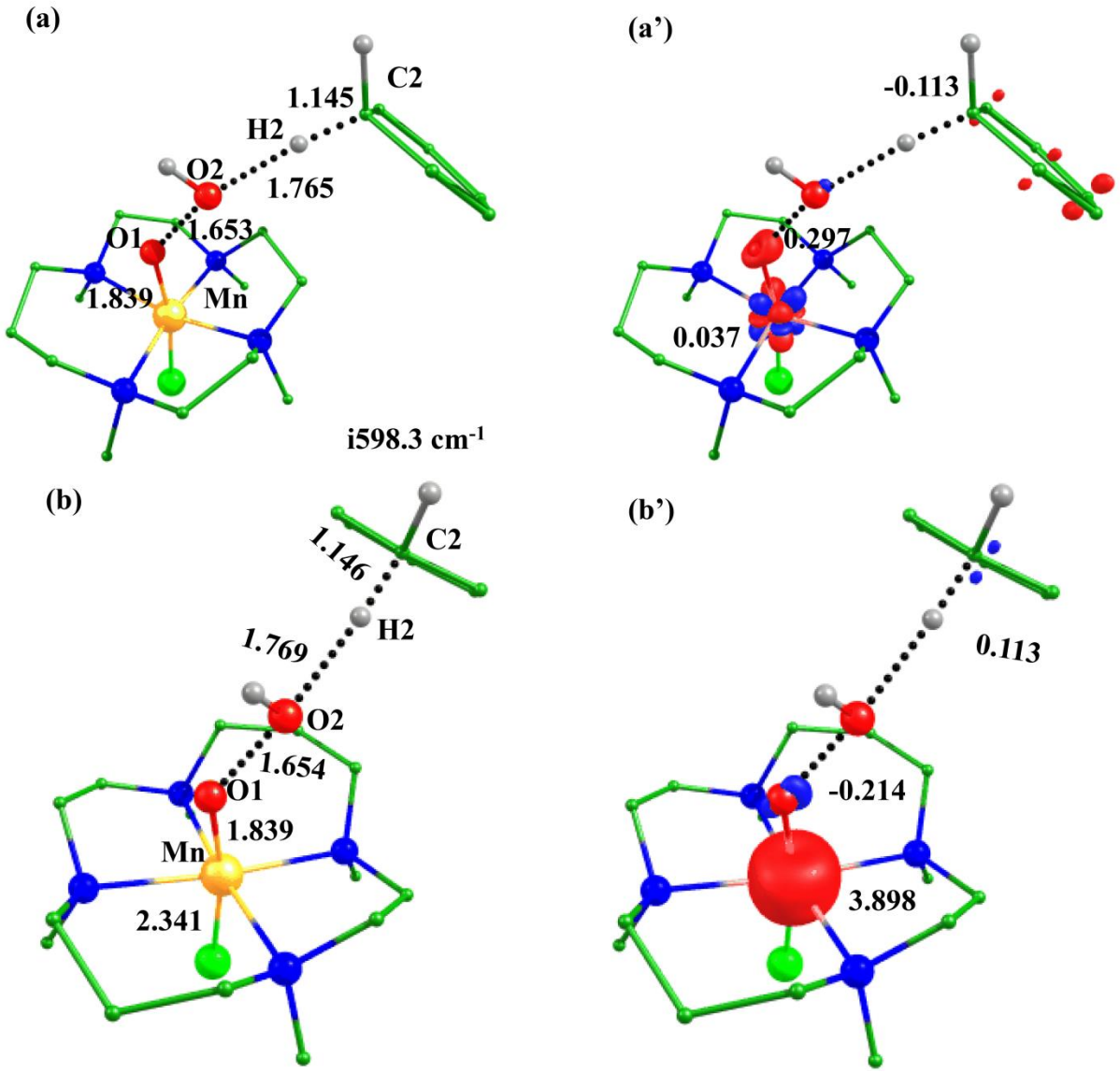

Fig. S8 B3LYP-D2 a) optimized structure (bond lengths in Å), a') corresponding spin density plot of $^{4}III_{a\text{-}is}$-ts2, b) optimized structure and b') corresponding spin density plot of $^{4}III_{b\text{-}is}$-ts2.

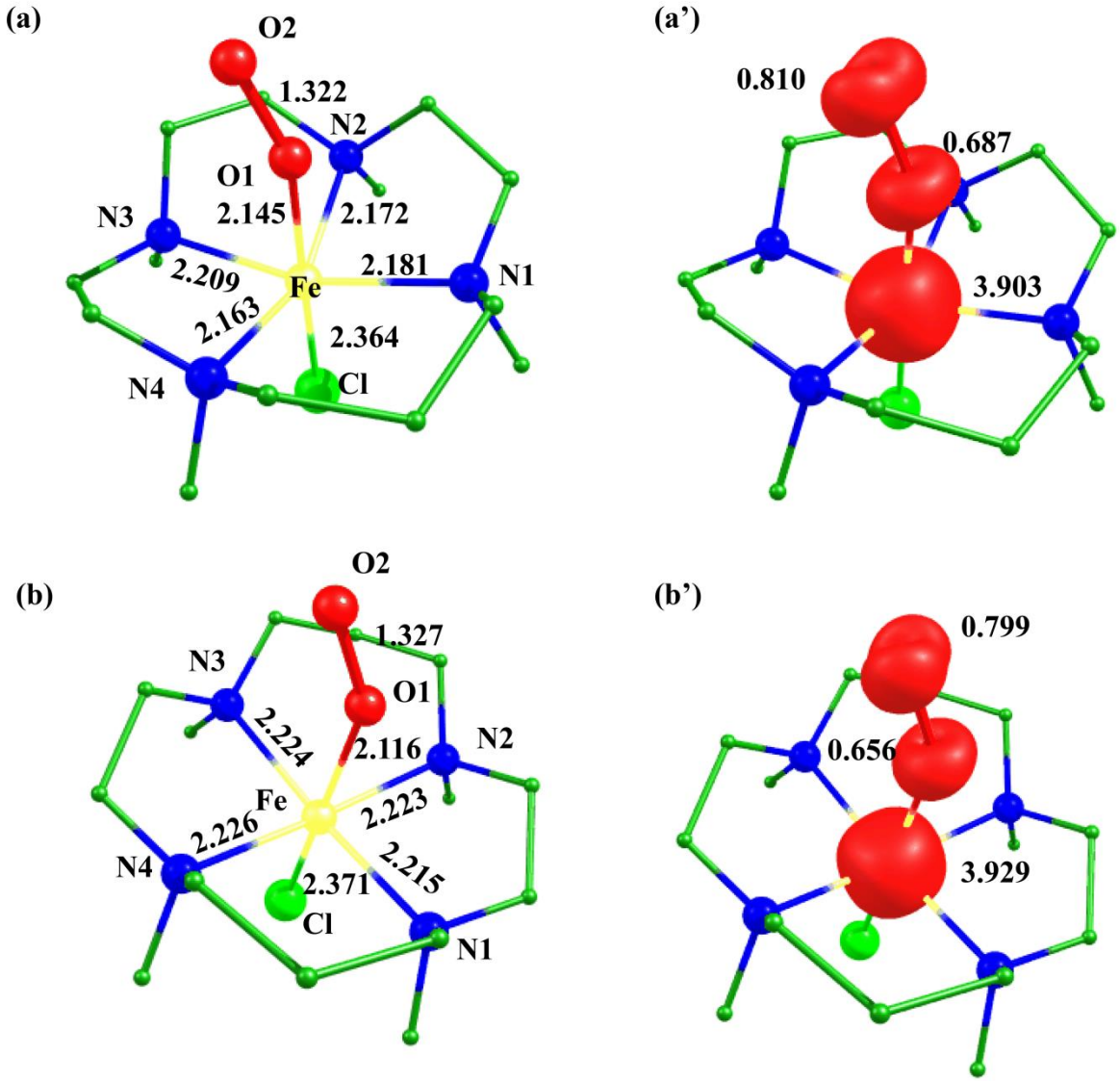

Fig. S9 B3LYP-D2 a) optimized structure (bond lengths in Å), a') corresponding spin density plot of $^{7}IV_{a\text{-}hs}$, b) optimized structure (bond lengths in Å) and b') corresponding spin density plot of $^{7}IV_{b\text{-}hs}$.

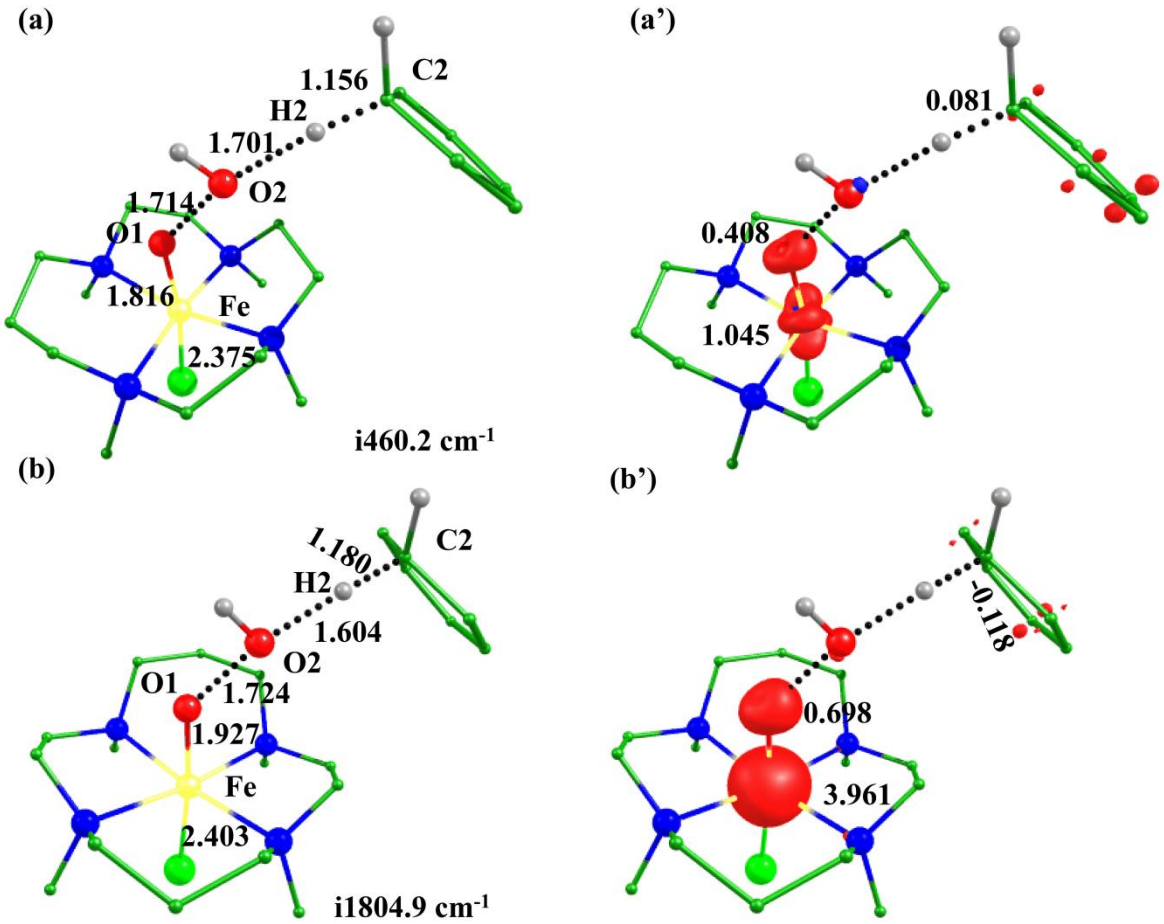

Fig. S10 B3LYP-D2 a) optimized structure (bond lengths in Å), a') corresponding spin density plot of $^{3}IV_{a\text{-}ls}$-ts2, b) optimized structure (bond lengths in Å) and b') corresponding spin density plot of $^{7}IV_{b\text{-}hs}$-ts2.

Here, we have got optimized geometry only at low spin surface of species V and other surfaces could not get optimize due to convergence issue. So we have performed the single point calculation for the other spin surfaces using co-ordinates of optimized geometry of the low spin state. Our results show that low spin of species V is the ground state.

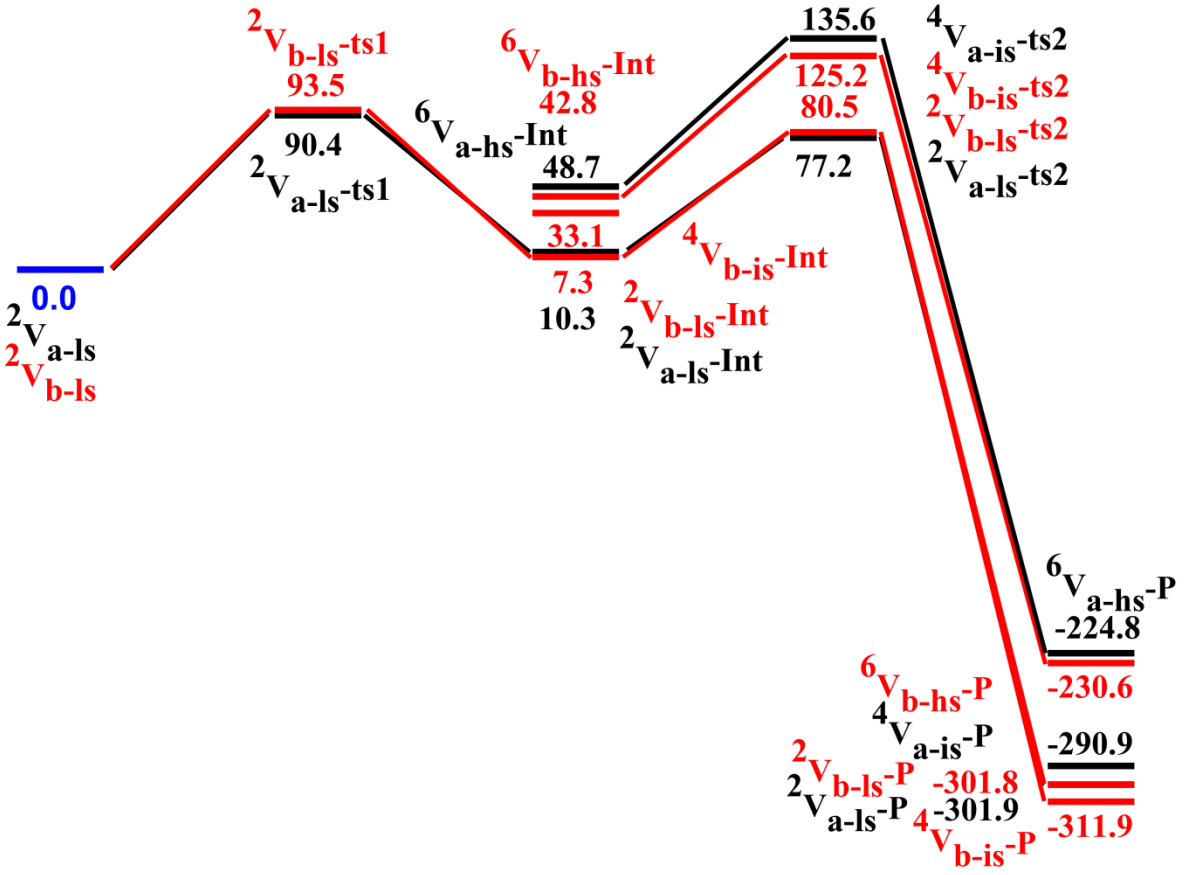

Fig. S11 B3LYP-D2-computed energy surface (ΔG in kJmol^{-1}) for C-H activation by cobalt-superoxo species (13-TMC (black), 14-TMC (red).

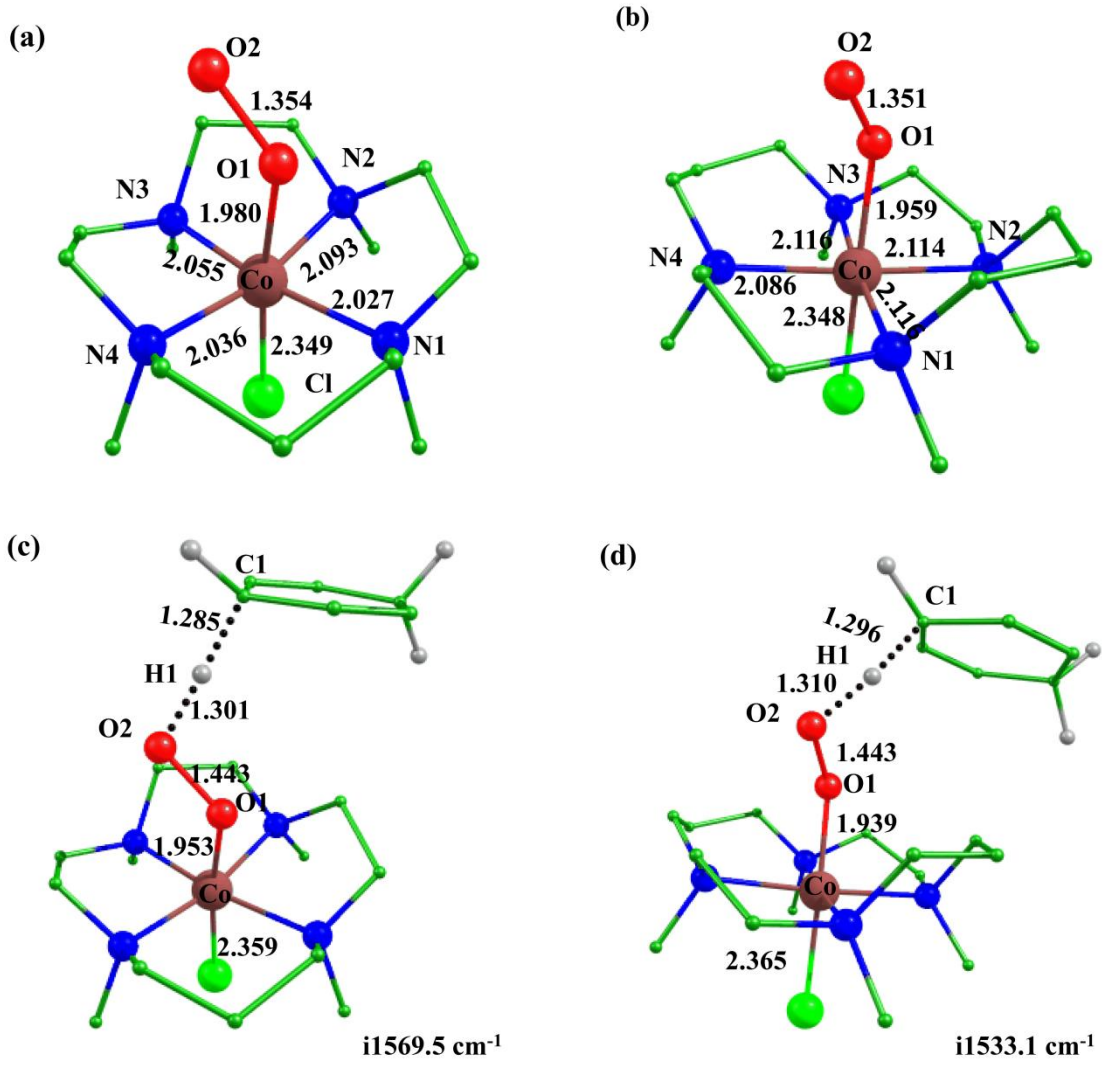

Fig. S12 B3LYP-D2 a) optimized structure (bond lengths in Å) of $^{2}V_{a\text{-}ls}$, b) optimized structure (bond lengths in Å) of $^{2}V_{b\text{-}ls}$, B3LYP-D2 c) optimized structure (bond lengths in Å) of $^{2}V_{a\text{-}ls}$-ts2, d) optimized structure (bond lengths in Å) of $^{2}V_{b\text{-}ls}$-ts2.

References

1. M. Q. E. Mubarak, S. P. de Visser, *Dalton Trans.*, 2019, **48**, 16899-16910.
2. J. B. Gordon, A. C. Vilbert, M. A. Siegler, K. M. Lancaster, P. Moenne-Loccoz, D. P. Goldberg, *J. Am. Chem. Soc.*, 2019, **141**, 3641-3653.
3. B. Wang, Y.-M. Lee, W.-Y. Tcho, S. Tussupbayev, S.-T. Kim, Y. Kim, M. S. Seo, K.-B. Cho, Y. Dede, B. C. Keegan, T. Ogura, S. H. Kim, T. Ohta, M.-H. Baik, K. Ray, J. Shearer, W. Nam, *Nat. Commun.*, 2017**,** **24**, 14839-14849.
4. J. Cho, J. Woo, W. Nam, *J. Am. Chem. Soc.*, 2010, **132**, 5958-5959.
5. J. Cho, J. Woo, W. Nam, *J. Am. Chem. Soc.*, 2012, **134**, 11112-11115.
6. J.-U. Rohde, J.-H. In, M. H. Lim, W. W. Brennessel, M. R. Bukowski, A. Stubna, E. Munck, W. Nam, L. Que, Jr., *Science*, 2003, **299**, 1037-1039.